中国航空学会 Chinese Society of Aeronautics and Astronautics
IAGA INTERNATIONAL ASSOCIATION FOR GREEN AVIATION
ICGA 2026 2026 INTERNATIONAL CONFERENCE ON GREEN AVIATION
XI' AN,CHINA NOV.1-3, 2026

Deep Learning-Based Wake Reconstruction for Vortex-Induced Vibrations in a Flexible Flag System

Invited lecture: machine learning for flow–structure problems in green aviation

Dr Zaib Ali
Department of Mechanical Engineering, School of Mechanical and Manufacturing Engineering (SMME)
National University of Sciences and Technology (NUST), Islamabad, Pakistan

Track 4: Aviation Digitalization and Intelligence Forum · Nov. 3, 2026, 15:00–15:30 · Jianzhang Hall 2

Why this topic matters for ICGA 2026

Fits Track 4 (Aviation Digitalization and Intelligence): AI-driven design, digital twins and high-fidelity simulation are exactly where learned surrogates sit.

Supports ICGA's goals: cheaper flow–structure analysis speeds up design exploration for efficient, low-emission systems, in line with the UN SDGs and ICAO LTAG.

Clean

Flexible flags in a wake harvest flow energy; a cheap surrogate cuts simulation effort per design.

Smart

A deep-learning surrogate that reconstructs wake fields in one forward pass: a digital-twin building block.

Safe

Wake and VIV signatures of flexible structures inform flutter and fatigue awareness.

Innovative

Mesh-free mask encoding and a gap-conditioned U-Net for a freely moving body.

Roadmap of the lecture

Part 1

Aviation context

Climate pressure and where flow–structure interaction appears in aircraft

Part 2

How FSI is computed

Coupling strategies, immersed boundaries and reduced-order models

Part 3

Machine learning today

PINNs, operators, graph networks, CNN surrogates and their use in FSI

Part 4

Case study and outlook

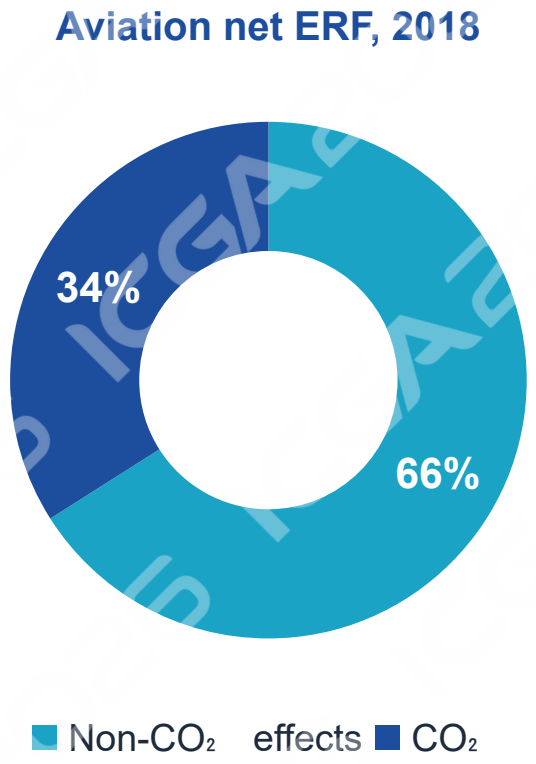
Wake reconstruction behind a bluff body with a flexible flag, and the road to aviation

Part 1 · Aviation's climate challenge

3.5 %
of net anthropogenic ERF from aviation, 2011 (Lee et al., 2021)

≈ 3×
warming vs. CO_2 alone (GWP* analysis) (Lee et al., 2021)

2050
ICAO LTAG: net-zero CO_2 (ICAO, 2022)



Implication

Net-zero by 2050 needs new configurations, propulsion and fuels, each evaluated through many coupled simulations. Faster, trustworthy analysis shortens that loop.

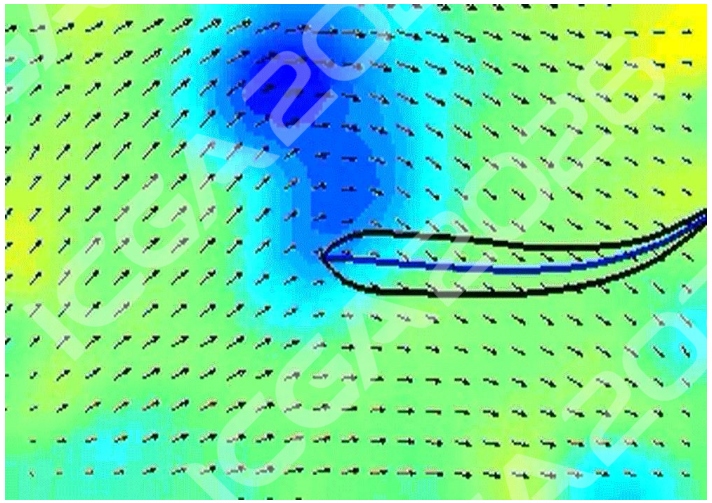
Sources: Lee et al. (2021): 66 % non-CO_2 share (2018); CO_2 share = 100 % − 66 %.

Part 1 · Where flow–structure interaction matters in aviation

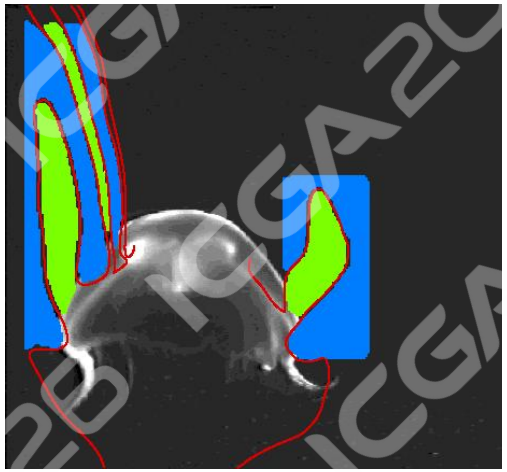
Phenomenon	Why it matters in aviation	Key literature
Flutter and limit-cycle oscillations	Aeroelastic stability of wings and control surfaces; active flutter suppression	(Dowell & Hall, 2001; Livne, 2018)
Vortex- and wake-induced vibration	Slender flexible components in bluff-body wakes: lock-in and fatigue	(Bearman, 1984; Williamson & Govardhan, 2004)
Flexible and morphing surfaces	Data-driven aeroelastic models for deforming wings and control	(Kou & Zhang, 2021; Hickner et al., 2021)
Flow-energy harvesting	Aeroelastic flutter harvesters as local power for sensors	(Bryant & Garcia, 2011; Abdelkefi, 2016)
Structural life and health	Airframe digital twin: flight loads → deflections → damage	(Tuegel et al., 2011; Glaessgen & Stargel, 2012)

Part 2 · Fluid Structure Interaction

Fluid-structure interaction: widespread in nature



Slaloming between vortices
Liao et al. (2003)



Jellyfish
Dabiri et al. (2005)

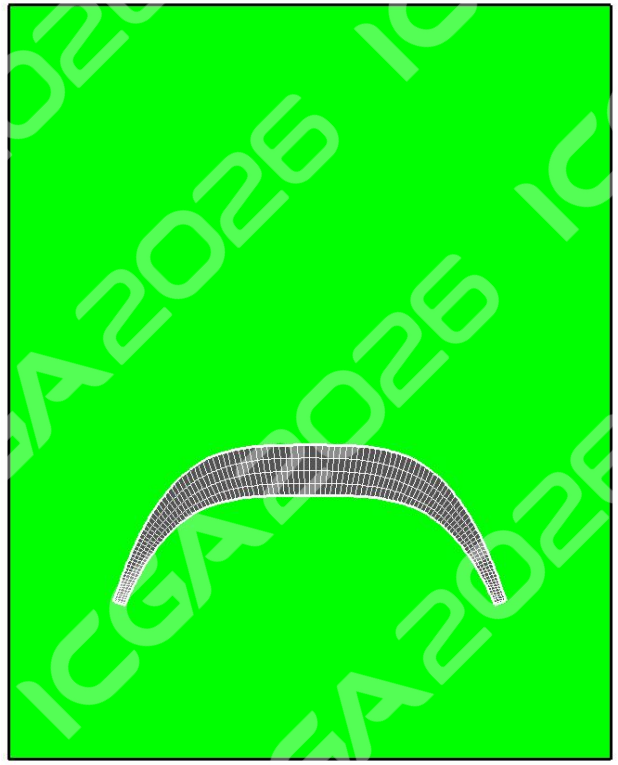


Trout behind obstacle
Liao et al. (2003)

Part 2 · Fluid Structure Interaction



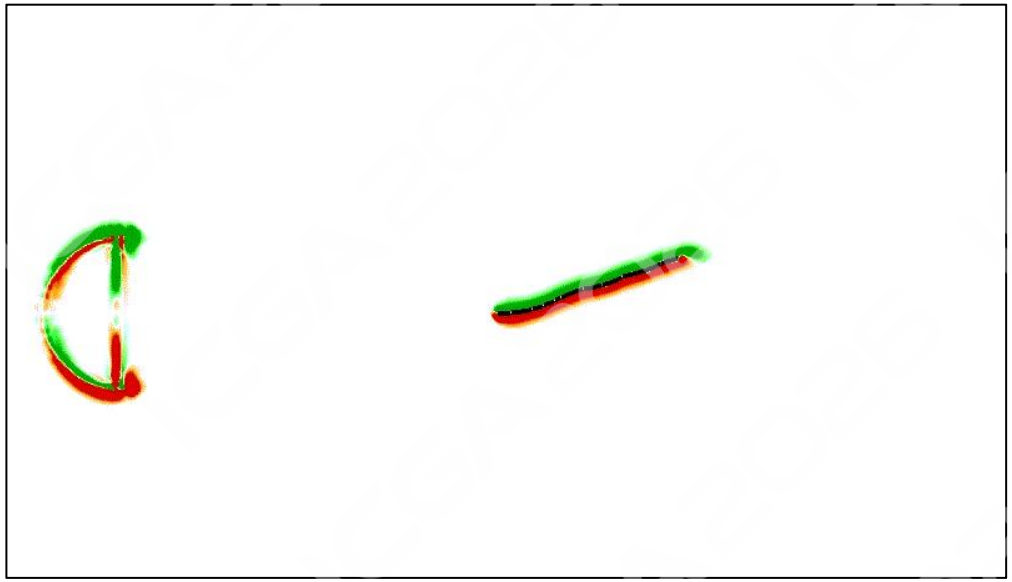
Re=300



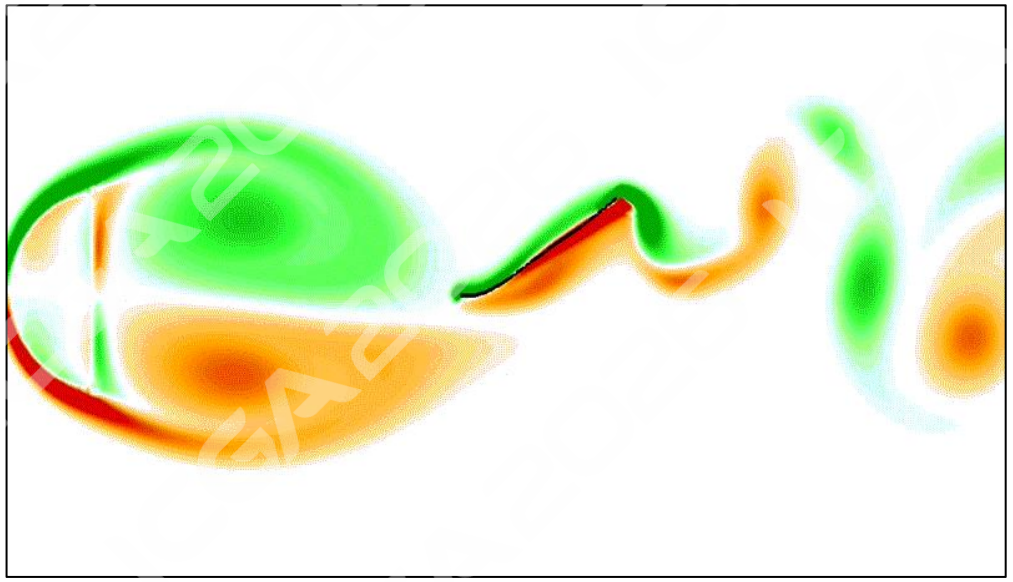
Re=800

Part 2 · Fluid Structure Interaction

Head fixed



Head movement with shedding frequency



Part 2 · How flow–structure problems are computed

Coupling strategy

Monolithic

One coupled system; robust but complex to build

Partitioned

Separate solvers; modular, but added-mass instability

Spatial discretisation

Conforming

Body-fitted ALE meshes; accurate at the wall, remeshing for large motion

Immersed boundary

Moving bodies on fixed grids; less accurate at the interface

> 10,000

CPU hours quoted for a coupled FSI case (Ong & Yin, 2025)

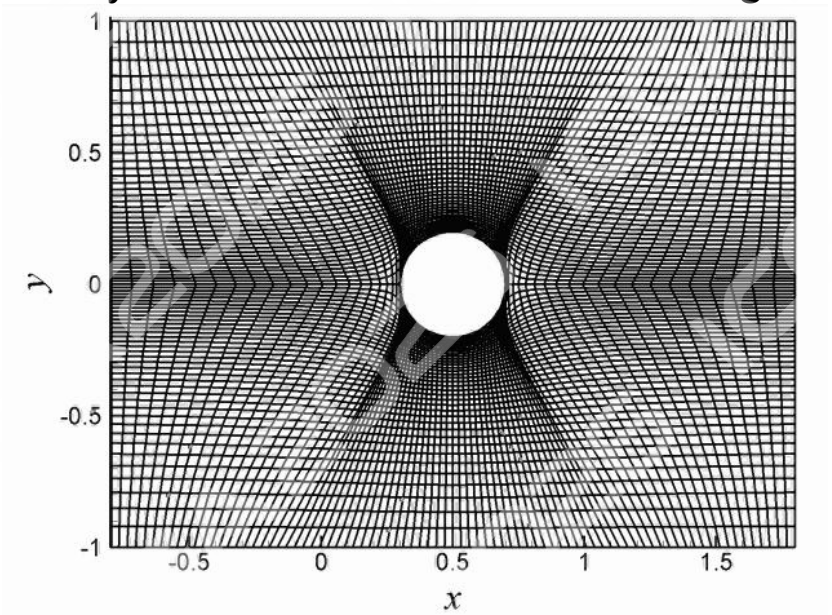
This study's 2D cases: ≈ 8 h each (8-core workstation)

Many design points × many conditions → surrogates

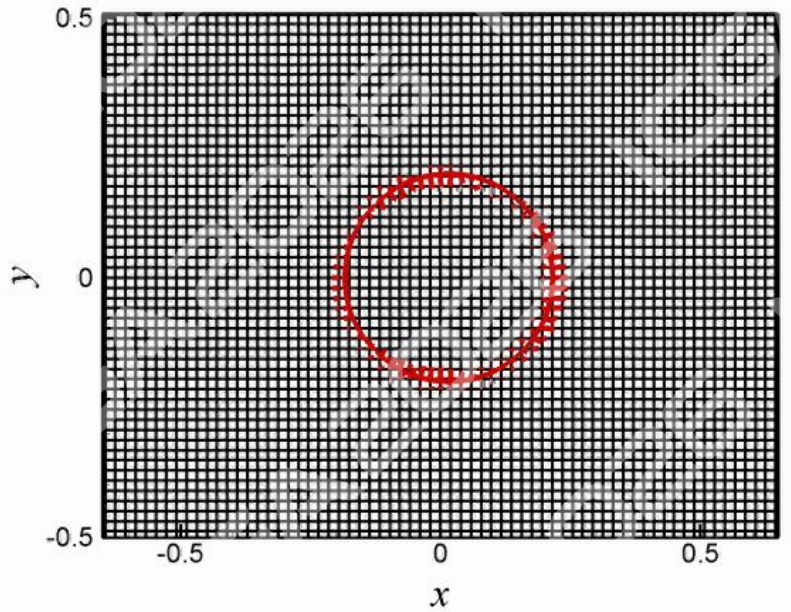
Reviews: (Dowell & Hall, 2001; Hou et al., 2012); added-mass effect: (Causin et al., 2005); immersed boundary method: (Peskin, 2002).

Part 2 · Fluid Structure Interaction

Body-fitted meshes, unstructured grid



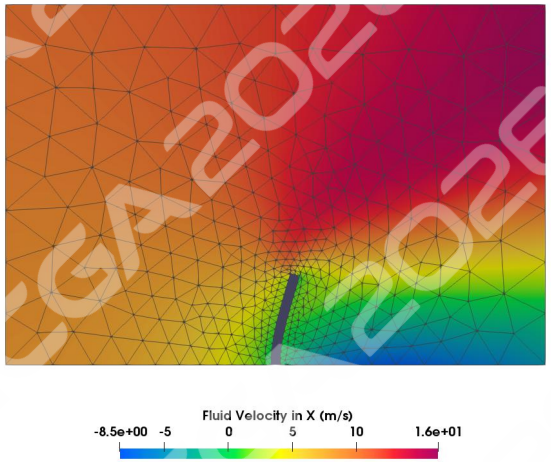
IBM, structured grid



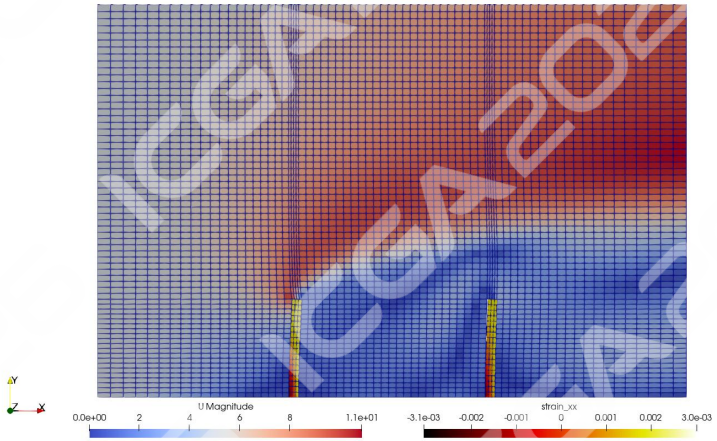
Need for interpolation and grid regeneration

Easy grid generation, Easy coding, Saving CPU time

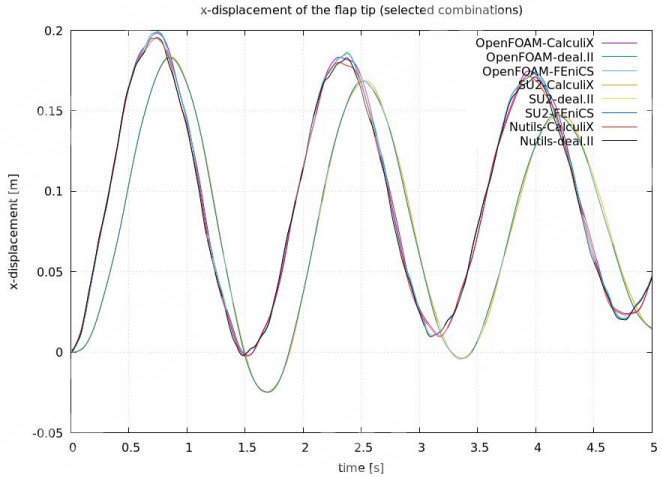
Part 2 · FSI test cases (1/3): flexible flaps in channel flow



Single flap: fluid velocity (x), flap deflected by flow



Two flaps, fluid + two solids, implicit multi-coupling

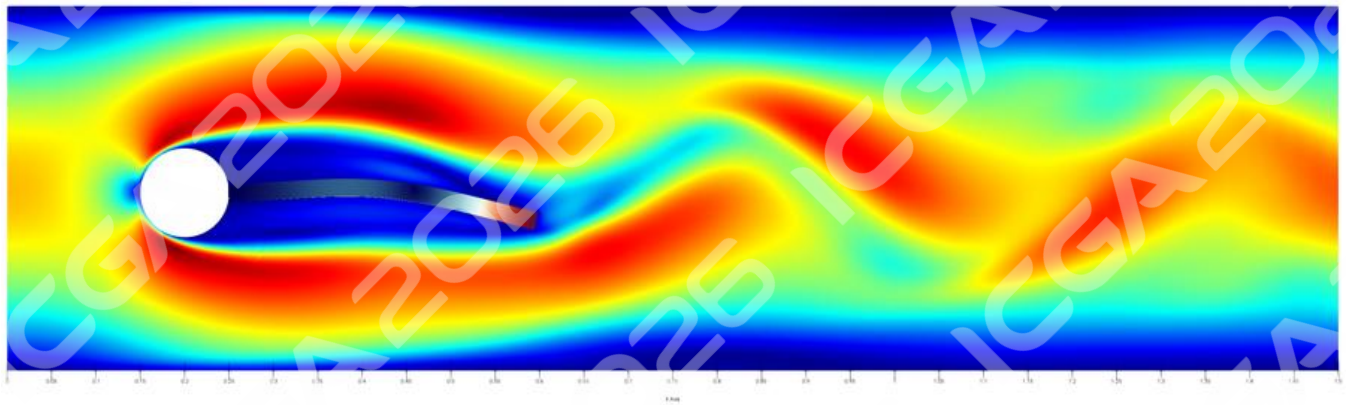


Flap-tip x-displacement for several fluid–solid solver pairs

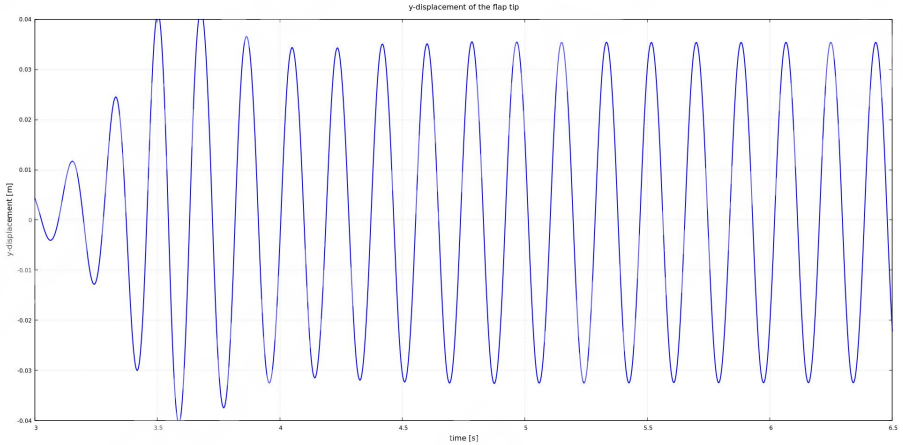
- Elastic flap fixed to a channel floor, oscillating under fluid pressure; coupled solvers (e.g. OpenFOAM, SU2, CalculiX, deal.II) (Chourdakis et al., 2022)
- Flap-tip displacement from different solver pairs agrees closely: such cases verify coupling codes (preCICE, n.d.)

Figures: preCICE tutorials, perpendicular-flap and multiple-perpendicular-flaps (LGPL-3.0) (preCICE, n.d.).

Part 2 · FSI test cases (2/3): Turek–Hron beam behind a cylinder



FSI3 case: flow past a cylinder with a flexible beam (velocity field)

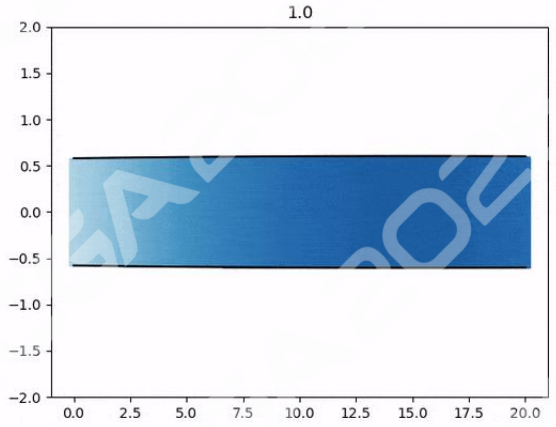


Beam-tip y-displacement versus time

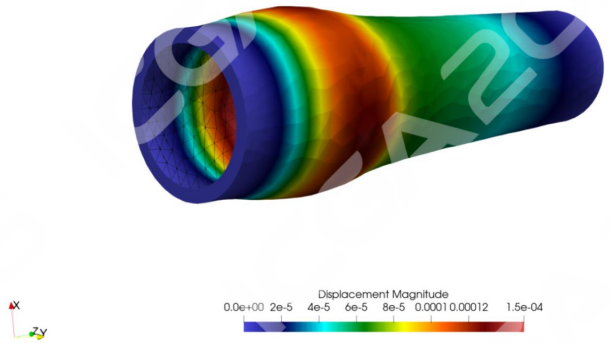
- Well-established benchmark of an elastic object in laminar incompressible flow (Turek & Hron, 2006); FSI3 is the hardest case for added mass (preCICE, n.d.)
- Same layout as our study: bluff body upstream, flexible tail downstream; ours adds the gap G_x as a parameter
- Large-amplitude, nearly periodic tip motion: the kind of response a surrogate must reproduce

Figures: preCICE tutorial turek-hron-fsi3 (LGPL-3.0) (preCICE, n.d.).

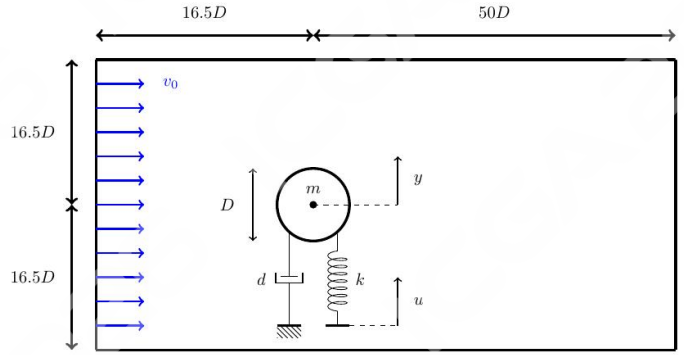
Part 2 · FSI test cases (3/3): elastic tubes and moving cylinders



1D elastic tube (animation)



3D expanding tube: displacement magnitude



Cylinder on spring–damper: VIV set-up

- Internal flow in a flexible tube (1D and 3D): pressure waves and wall displacement (preCICE, n.d.)
- Spring-mounted cylinder: shedding vortices drive the oscillation, the textbook VIV configuration (Williamson & Govardhan, 2004)

Figures: preCICE tutorials elastic-tube-1d / elastic-tube-3d / flow-around-controlled-moving-cylinder (LGPL-3.0) (preCICE, n.d.).

Part 2 · Reduced-order models: powerful, but linear

Modal decomposition

- POD and modal analysis of flow snapshots (Taira et al., 2017)
- Model reduction for flow analysis and control (Rowley & Dawson, 2017)

DMD and Koopman

- Dynamic mode decomposition for experimental and numerical data (Schmid, 2010)
- Deep autoencoders learn Koopman embeddings (Lusch et al., 2018)

Aeroelastic ROMs

- Reduced-order modelling for computational physics (Lucia et al., 2004)
- ROM interpolation applied to aeroelasticity (Amsallem & Farhat, 2008)

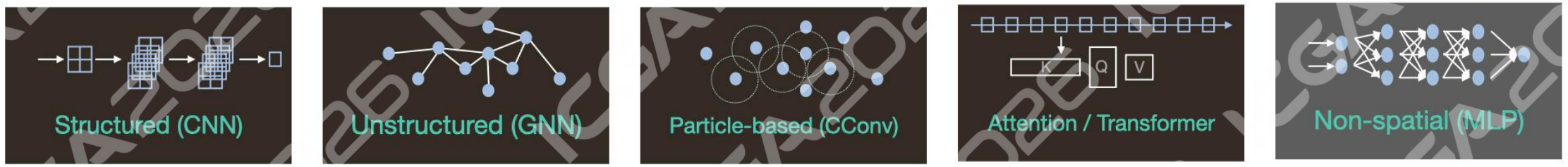
Limit: linear subspaces struggle with broadband nonlinear wakes and transitional regimes, which motivates learned nonlinear models.

Part 3 · ML for fluid mechanics: a short timeline

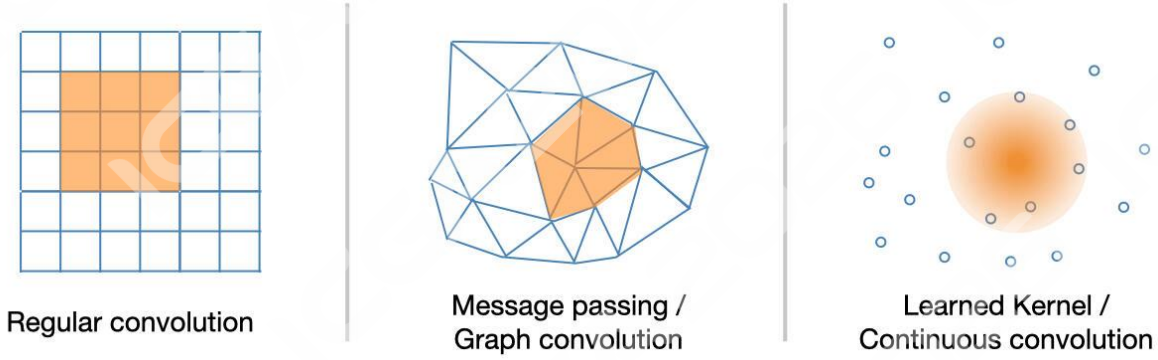
2015–16	2018–19	2020	2021	2024	2025
U-Net (Ronneberger et al., 2015); CNNs for steady flow (Guo et al., 2016)	Koopman autoencoders (Lusch et al., 2018); PINNs (Raissi et al., 2019b); deep learning of VIV (Raissi et al., 2019a)	Hidden fluid mechanics (Raissi et al., 2020); graph simulators (Sanchez-Gonzalez et al., 2020); RANS CNNs (Thuerey et al., 2020)	Neural operators (Lu et al., 2021; Li et al., 2021); MeshGraphNets (Pfaff et al., 2021); ML-accelerated CFD (Kochkov et al., 2021)	GNN reduced models for fluid–structure systems (Gao & Jaiman, 2024)	Inverted-foil GNN (Parekh et al., 2025); PINN + immersed boundary (Farea et al., 2025)

Overviews: (Brunton et al., 2020; Vinuesa & Brunton, 2022; Duraisamy et al., 2019; Kutz, 2017).

Part 3 · Which ML technique for which data?



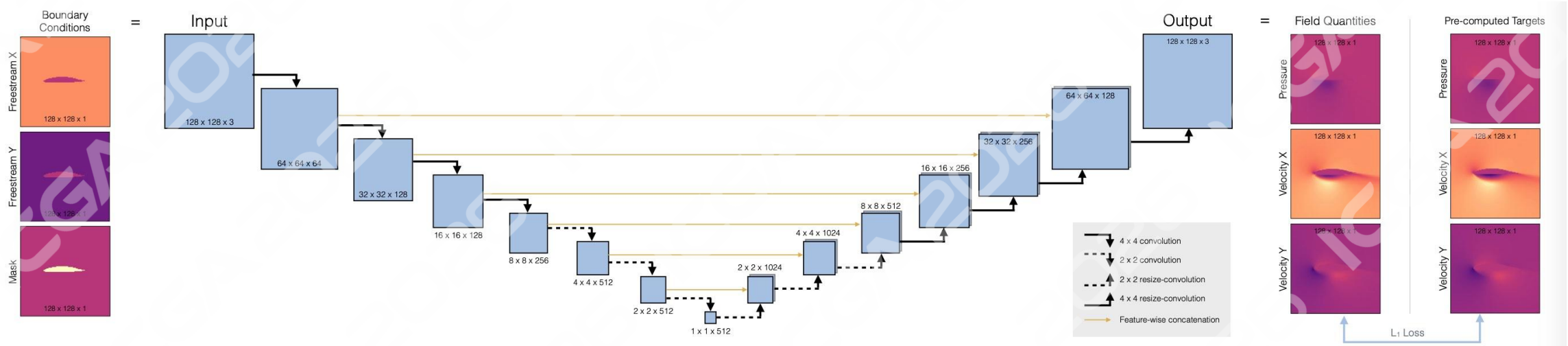
Network families by data layout (grid, mesh, particles, attention, coordinates). Figure: Thuerey et al. (2021).



- **CNN / U-Net:** structured grids; our case (Thuerey et al., 2020)
- **GNN:** moving, unstructured meshes (Gao & Jaiman, 2024)
- **MLP / PINN:** coordinates, scattered data (Raissi et al., 2019a)

Convolution on a grid, on a mesh (message passing) and on particles. Figure: Thuerey et al. (2021).

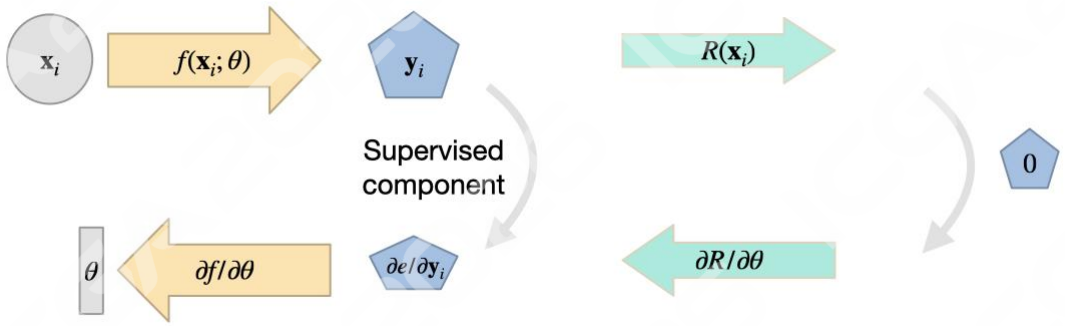
Part 3 · The U-Net surrogate: architecture



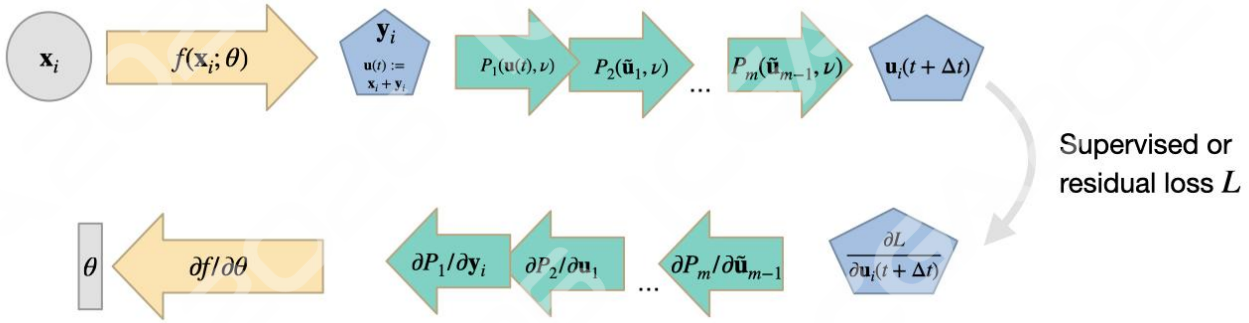
U-Net for RANS airfoil flow: free-stream and airfoil mask in (left), pressure and velocity fields out (right). Figure: Thuerey et al. (2021); network: Thuerey et al. (2020).

- Geometry enters as an image channel (mask), outputs are full fields in one forward pass
- Encoder–decoder with skip connections (Ronneberger et al., 2015); our model adds gap conditioning through FiLM (Perez et al., 2018)

Part 3 · Physics-informed and differentiable physics



Physical-loss (PINN-type) learning: residual R of the governing equation in the loss. Figure: Thuerey et al. (2021).

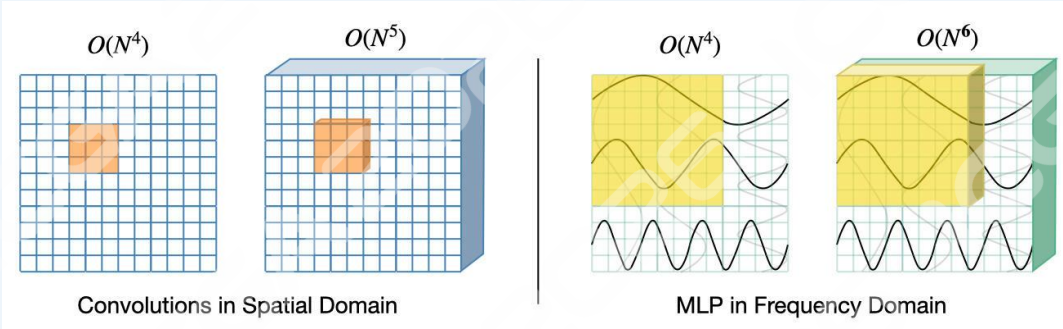


Differentiable physics: gradients flow through a solver. Figure: Thuerey et al. (2021).

- PINNs embed PDEs in the loss (Raissi et al., 2019b; Cai et al., 2021)
- Hidden fluid mechanics: fields from visualisations (Raissi et al., 2020)
- VIV: Navier–Stokes + structure equation, pressure from sparse data (Raissi et al., 2019a)
- PINN + immersed boundary for moving solids (Farea et al., 2025)

Part 3 · Neural operators and graph networks on wings

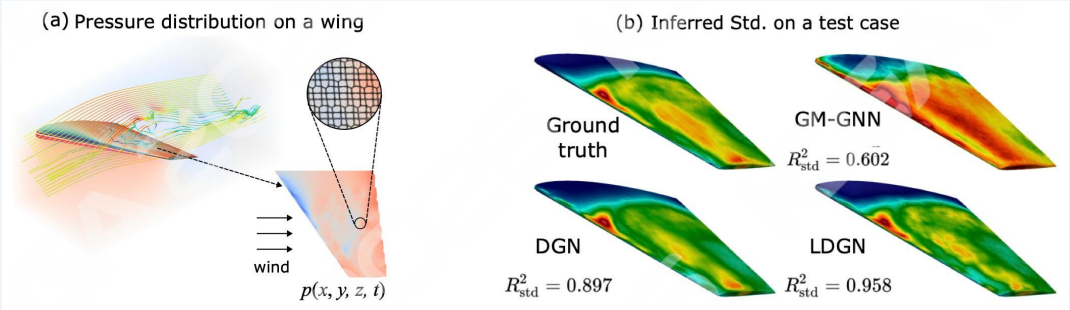
Fourier neural operator



Spatial convolution vs. learned multiplication in the frequency domain. Figure: Thuerey et al. (2021).

Global receptive field, parametric PDEs (Li et al., 2021; Lu et al., 2021)

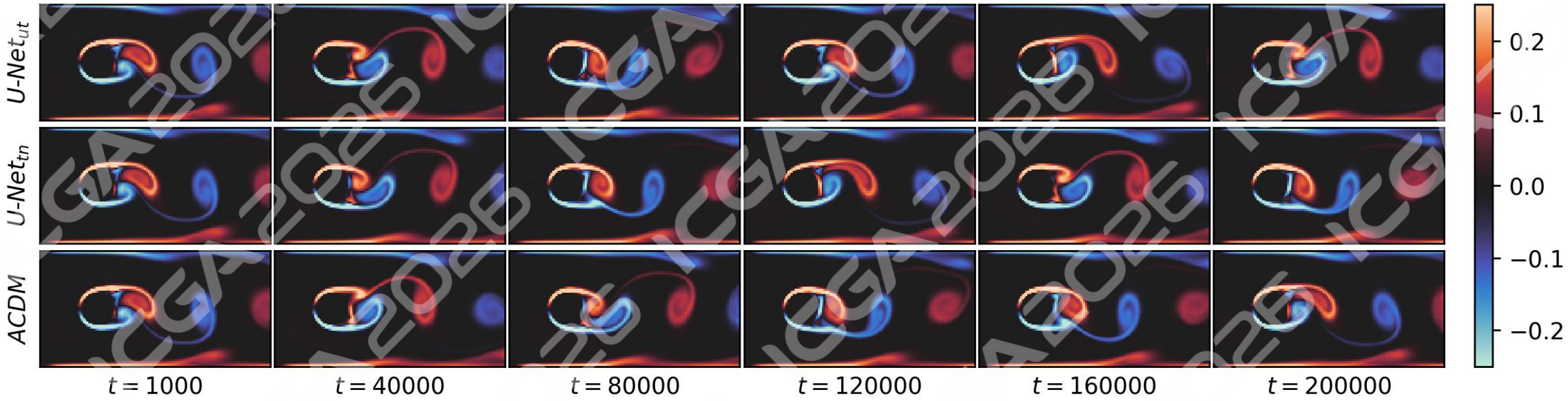
Graph networks on a 3D wing



Pressure statistics on a 3D wing, ground truth vs. graph models. Figure: Thuerey et al. (2021); method: Lino et al. (2025).

Meshes follow geometry; wing example (Pfaff et al., 2021; Lino et al., 2025)

Part 3 · Wake dynamics with autoregressive models



Vorticity predictions for an incompressible wake flow (Re = 1000) over 200,000 time steps: U-Net variants (rows 1–2) and ACDM (row 3). Figure: Thuerey et al. (2021); method: Kohl et al. (2023).

- Autoregressive and diffusion surrogates roll out vortex shedding stably when the flow is periodic
- Transitional regimes remain harder, as in our own error analysis

Part 3 · CNN and U-Net surrogates for flow fields



Airfoil RANS flow (p, V_x, V_y): target solution (left) vs. CNN inference (right). Figure: Thuerey et al. (2020), from the authors' public code repository (Apache-2.0).

Steady flows

CNNs approximate steady flow and aerodynamic fields (Guo et al., 2016; Bhatnagar et al., 2019)

Unsteady wakes

Cylinder wakes, bluff bodies and nonlinear modes (Lee & You, 2019; Hasegawa et al., 2020; Murata et al., 2020)

Reconstruction

Super-resolution of turbulent fields from coarse data (Fukami et al., 2019)

Part 3 · Machine learning for flow–structure systems

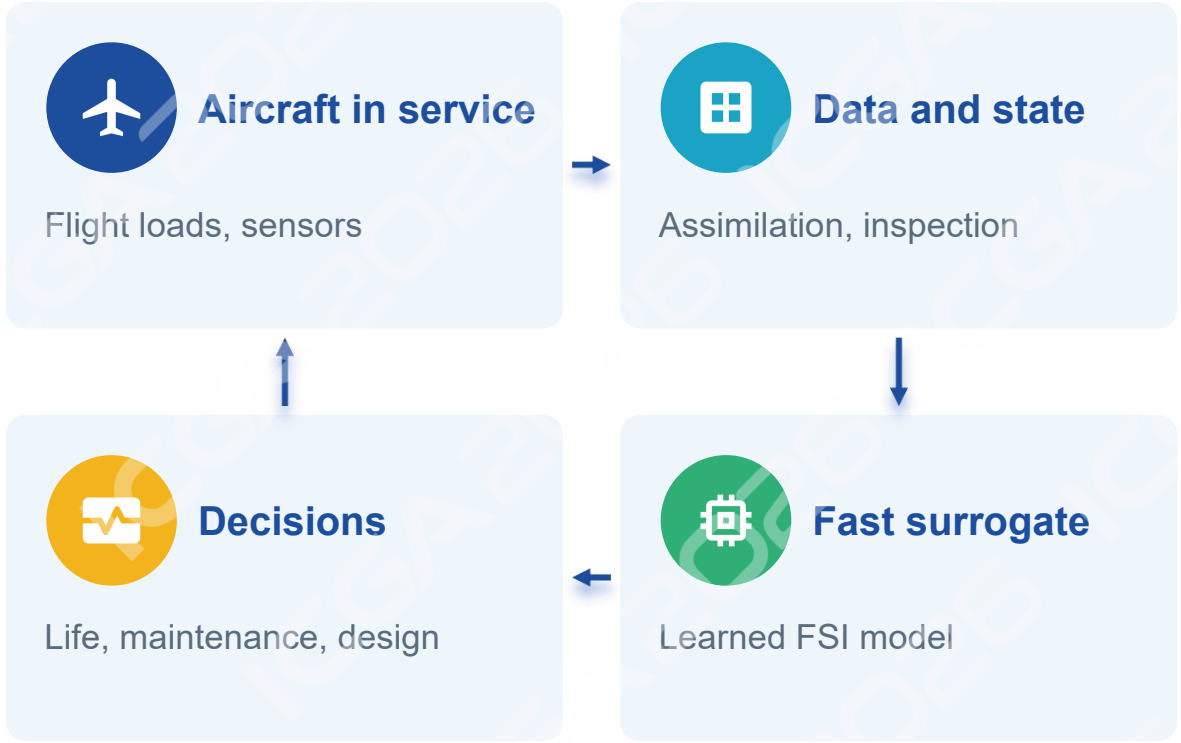
Study	Method	FSI case	Reported outcome
Raissi et al. (2019a)	PINN: Navier–Stokes + structure	Vortex-induced vibration of a cylinder	Pressure and structural parameters from scattered data
Miyanawala & Jaiman (2019)	POD + CNN	Freely vibrating bluff body	Long-time wake prediction
Gao & Jaiman (2024)	Hypergraph GNN reduced model (ALE)	Elastically mounted cylinder; hyperelastic plate	Quasi-monolithic; forces from predicted states
Farea et al. (2025)	Eulerian–Lagrangian PINN + IBM	2D cavity with a moving solid	Pressure error 12.9 % → 2.39 %
Parekh et al. (2025)	Hypergraph GNN surrogate	Inverted elastic foil (energy harvesting)	Long-horizon flapping prediction
This work	**Conditional U-Net + mask encoding**	**Flexible flag behind a D-shaped body, G_x = 0–2**	**Vorticity frames: pooled R^2 0.80, 41.5 % loss; per-gap R^2 0.12–0.80**

Part 3 · More ML studies on VIV and FSI

Study	Method	Case	Reported outcome
Cheng et al. (2021)	PINN with Navier–Stokes + structure equation	2-DOF VIV of a cylinder	Velocity, pressure and structural response from sparse data
Tang et al. (2022)	Transfer-learning PINN (TL-PINN)	Vortex-induced vibration	Accurate with progressively smaller datasets
Nazvanova et al. (2023)	POD + LSTM reduced-order model	VIV of a circular cylinder	Fast prediction of flow and structural response
Gupta & Jaiman (2022)	Hybrid partitioned deep learning (interface + flow networks)	Moving interface / FSI	Coupled interface and flow predictions
Bukka et al. (2021)	Hybrid deep-learning reduced-order models	Unsteady flow predictions	Assessment of ROMs that combine reduction and deep learning

Sources: studies from the thesis literature review; summaries paraphrase the pre-defence slides.

Part 3 · Digital twins in aircraft structures



- Tail-number-specific, ultra-high-fidelity model linking flight loads to deflection and damage (Tuegel et al., 2011)
- Digital-twin paradigm for future NASA and U.S. Air Force vehicles (Glaessgen & Stargel, 2012)
- GNN reduced models for FSI point to physics-based digital twins (Gao & Jaiman, 2024)
- A learned surrogate supplies the speed that real-time updating needs

Part 3 · Physics of our test case: wakes, inverted flags, harvesting

Bluff-body wakes and VIV

Lock-in occurs when shedding frequency nears a structural frequency (Williamson & Govardhan, 2004; Bearman, 1984)

Inverted flags

Large-amplitude flapping, interpreted as a vortex-induced vibration (Kim et al., 2013; Sader et al., 2016)

Flow-energy harvesting

Eel and flag harvesters; piezoelectric and inverted-flag designs (Allen & Smits, 2001; Michelin & Doaré, 2013; Shoele & Mittal, 2016)

Our dataset builds on Latif et al. (2023): an inverted flag in the wake of a cylindrical bluff body, simulated with an in-house immersed-boundary solver.

Part 4 · Positioning: what is established and what is open

Established

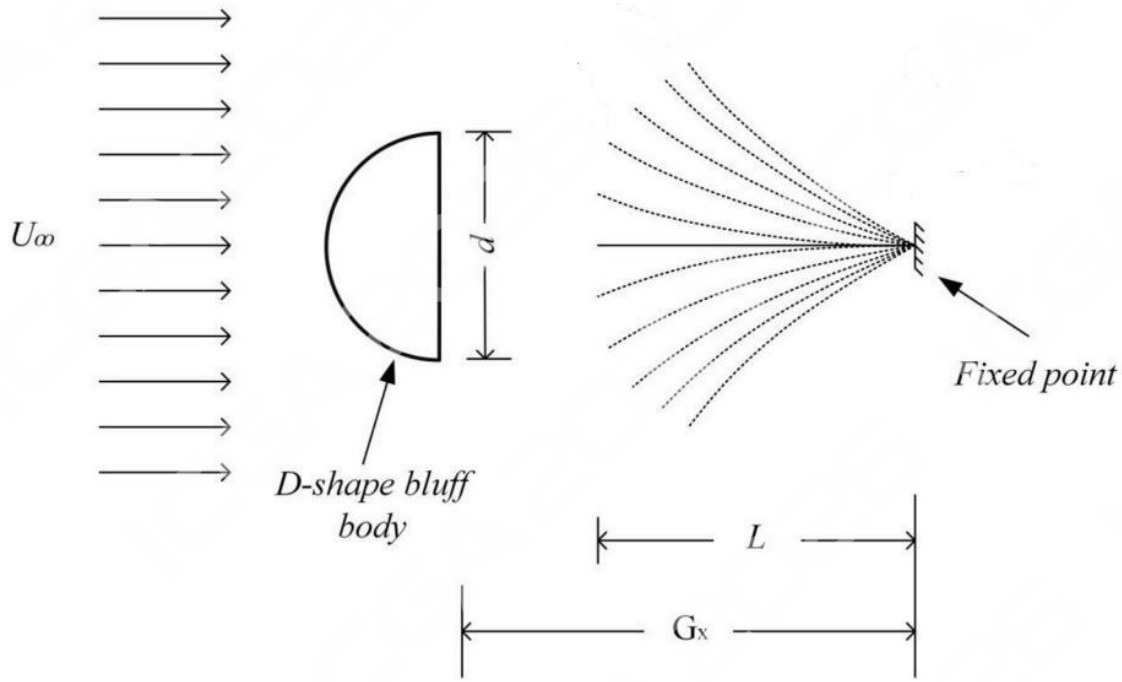
- Field-to-field CNN surrogates for flows (Thuerey et al., 2020)
- Physics-informed inference for VIV (Raissi et al., 2019a)
- Graph reduced models for FSI (Gao & Jaiman, 2024)

Open for grid-based models

- Compact input for a deforming, freely moving structure
- Explicit conditioning on a control parameter (the gap)
- Full vorticity-frame reconstruction, not only forces

This work: binary-mask encoding + gap-conditioned U-Net for vorticity reconstruction.

Case study · Test case and dataset

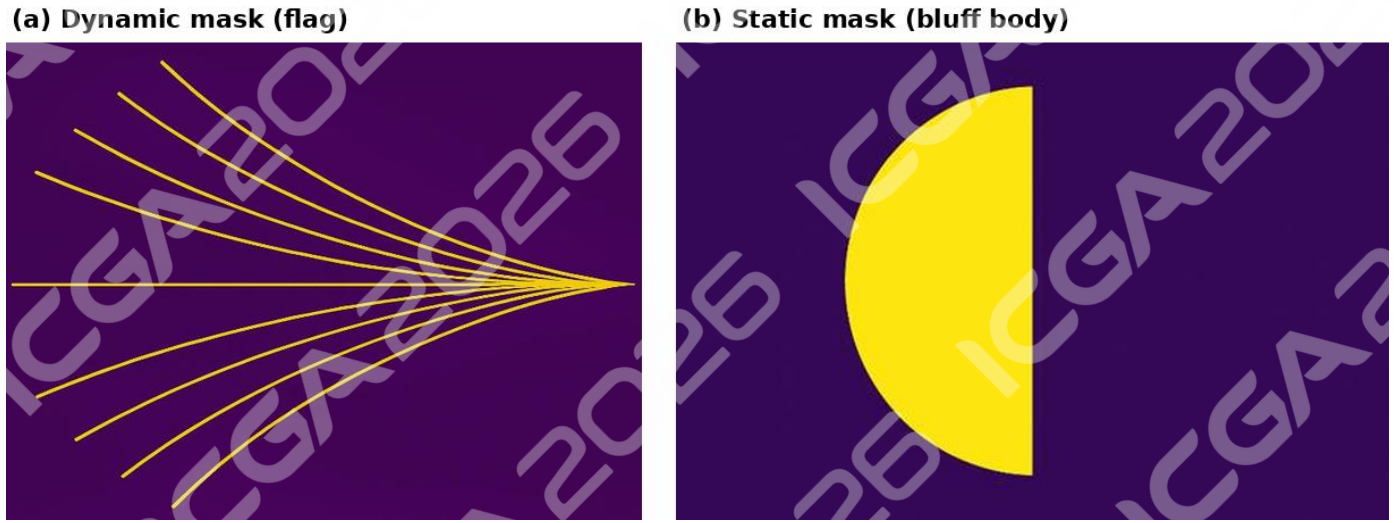


Set-up: bluff body (size d), clamped flag (length L), streamwise gap G_x.

Parameter	Value
Reynolds number	300
Bending coefficient	0.005
Gap G_x	0.00 – 2.00
Excluded gaps	0.20, 0.40, 1.20
Frames (train / test)	1040 / 160
Image size	512 × 512
Run time per case	≈ 8 h (8 cores)

Solver: in-house FORTRAN, immersed boundary
Basis: Latif et al. (2023)

Case study · Compact, mesh-free geometry encoding

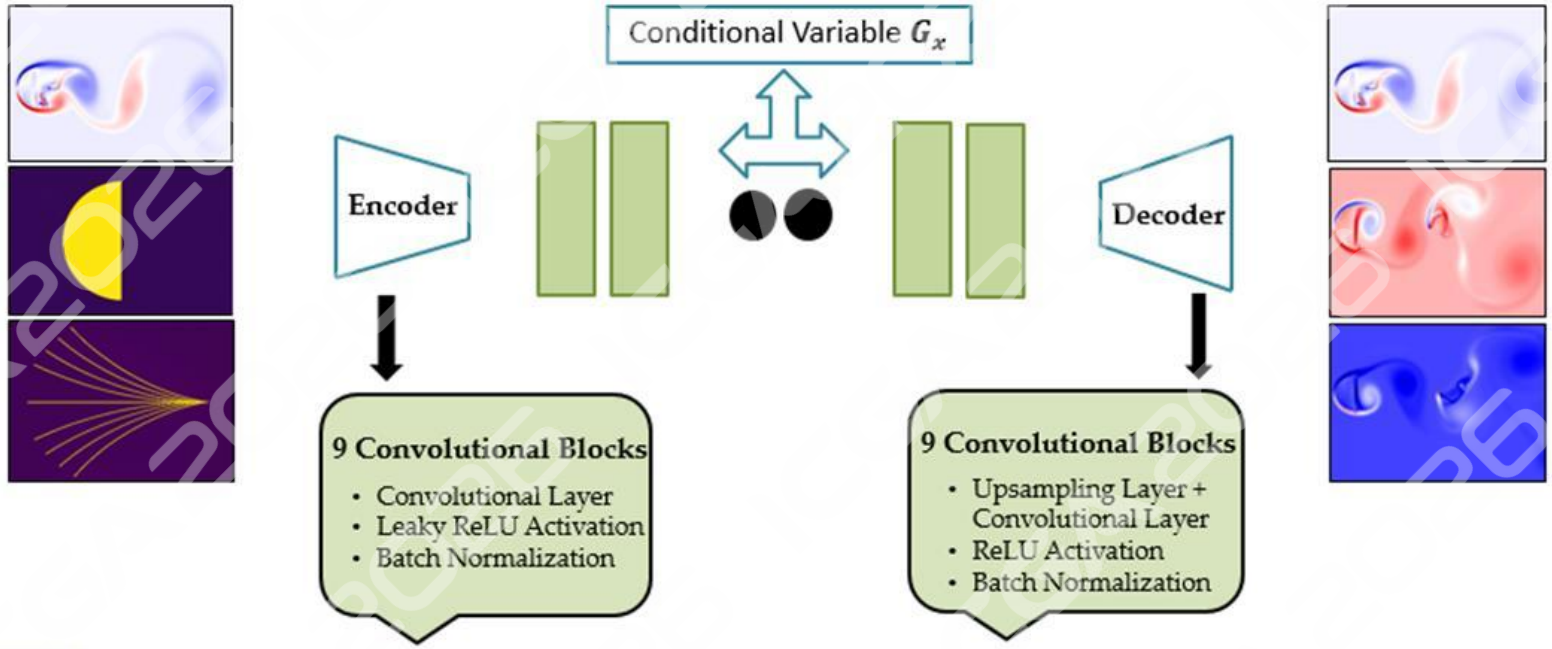


- No body-fitted mesh or remeshing for the moving flag
- Deforming geometry is a plain image channel for convolutions

Inputs and target

- **Input 1** bluff-body mask (static)
- **Input 2** flag mask (per frame)
- **Target** vorticity, scaled by max |ω|
- **Scalar** gap G_x (conditioning)

Case study · Conditional U-Net architecture



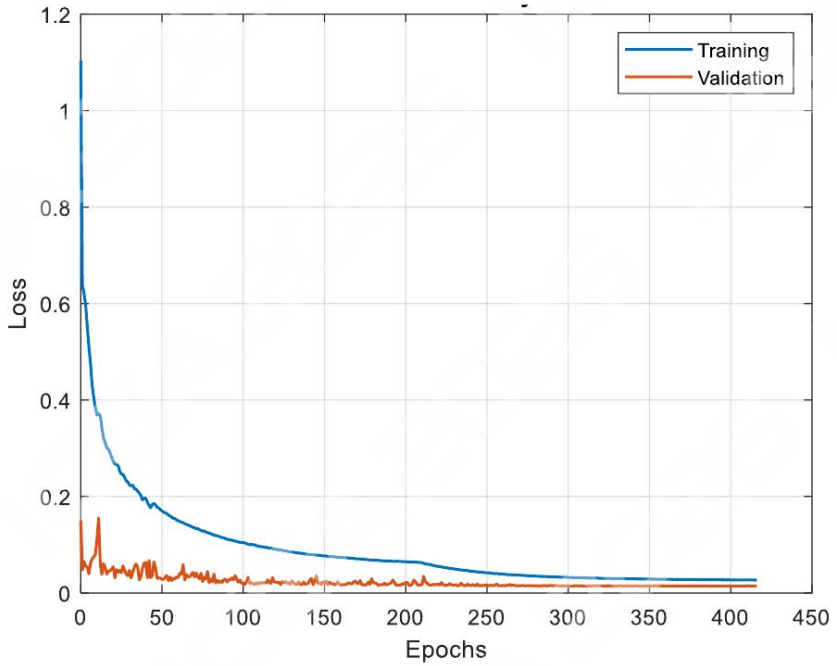
- 9 + 9 conv blocks with skip connections (Ronneberger et al., 2015)
- FiLM conditioning on G_x at the bottleneck (Perez et al., 2018)
- 5.38 M parameters, 32 base channels

Case study · Hybrid loss, training and convergence

Loss function

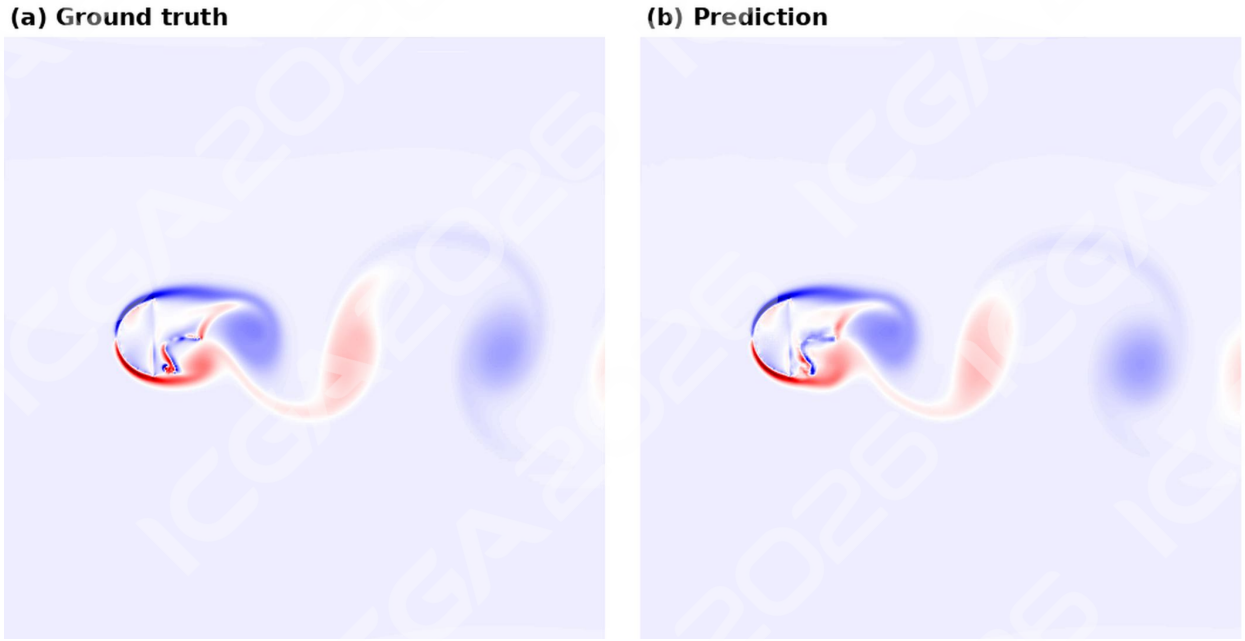
$$L_{total} = L_1 + \lambda L_{grad}$$

- L_1 pixel-wise absolute error
- L_{grad} gradient mismatch, in the spirit of (Mathieu et al., 2016)
- Adam (Kingma & Ba, 2015), lr 6×10^{-4} + decay, batch 5
- 80,000 iterations (417 epochs); 1040 train / 160 test frames



Final loss: train 0.0267 · validation 0.0144

Case study · Results: reconstructed wakes and headline accuracy



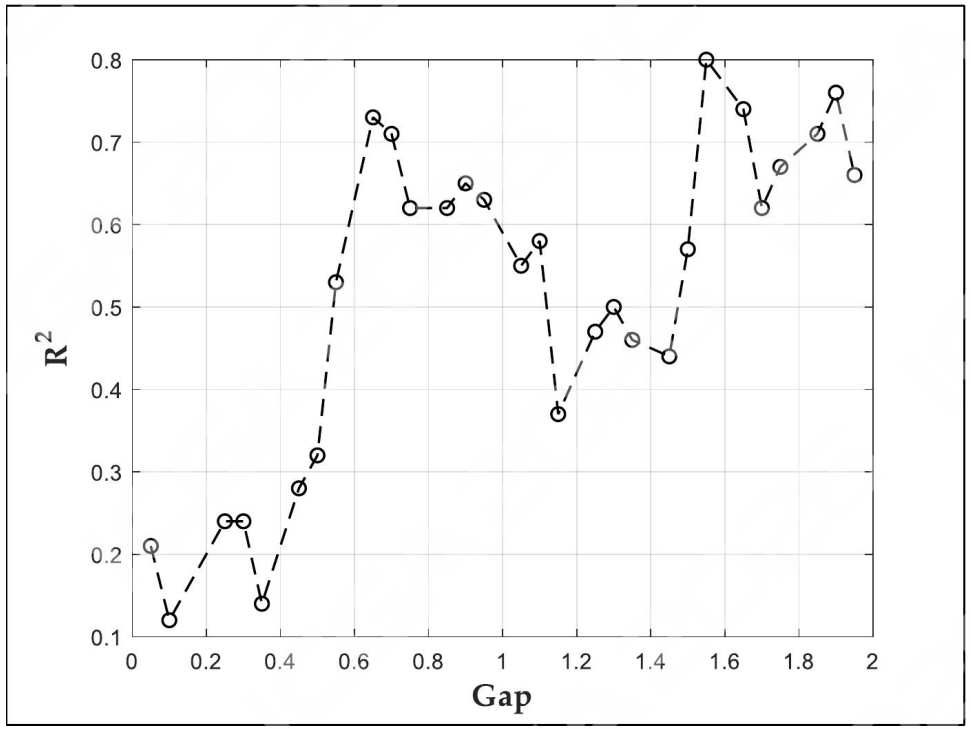
Red / blue: positive / negative vorticity. Figure: pre-defence results.

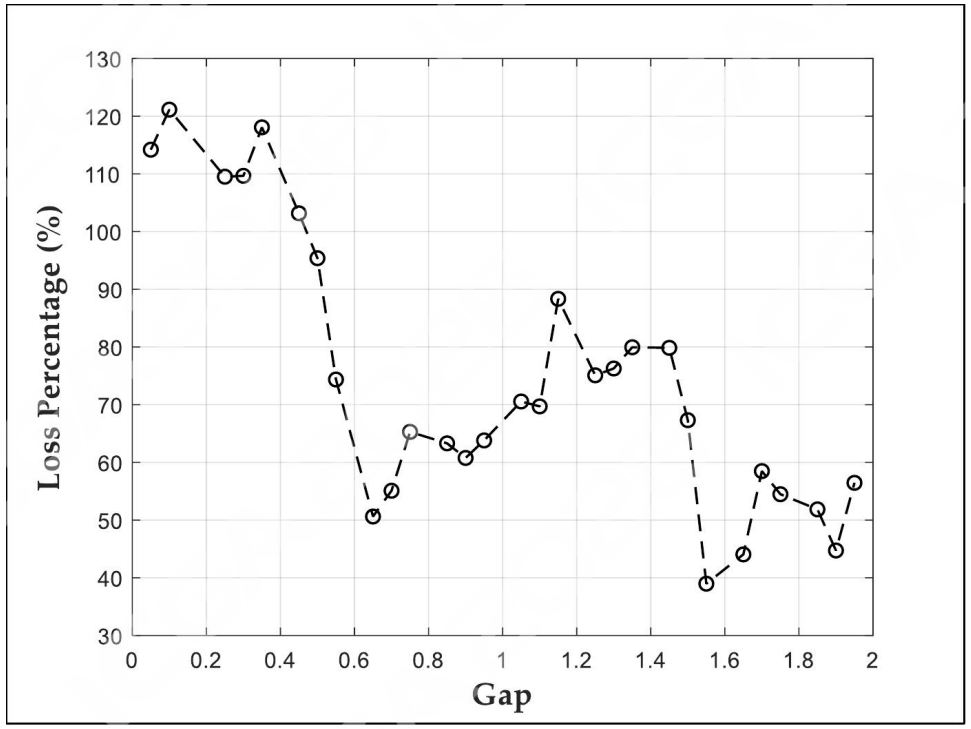
41.5 %
test loss (pooled)

0.80
R^2 (pooled)

- Large vortices and wake layout reproduced
- Per-gap R^2 spans 0.12–0.80 (mean ≈ 0.5)
- Test loss 78 → 51 → 42 % at epochs 122, 244, 417
- Width 8 → 16 → 32: 50 → 48 → 41 % loss

Case study · Per-gap results: R^2 and loss versus gap





R^2 spans 0.12–0.80 and loss 39–121 %: the pooled 0.80 hides a wide spread across flow regimes.

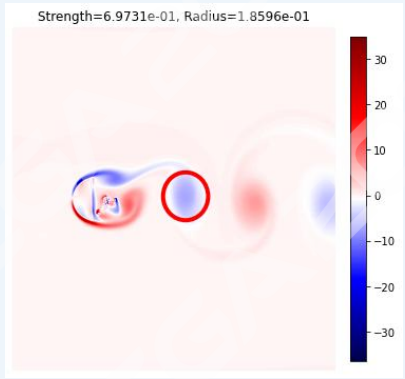
Case study · Gap regimes: where the model succeeds

G_x band	Avg R^2	Avg loss	Disturbed gap in band	Mean flag curvature	Avg vortex strength	Avg vortex radius	Verdict
0.05 – 0.50	0.22	110 %	Yes (0.20, 0.40)	0.274	0.75	0.19	**Fails**
0.55 – 0.95	0.64	62 %	No	0.208	0.76	0.21	**Works**
1.05 – 1.50	0.48	76 %	Yes (1.20)	0.217	0.91	0.22	**Partial**
1.55 – 1.95	0.71	50 %	No	0.221	0.33	0.08	**Works best**

Key finding: the two bands containing a turbulent gap are the two worst; the two without one are the two best. Flow regime, not gap size, decides success.

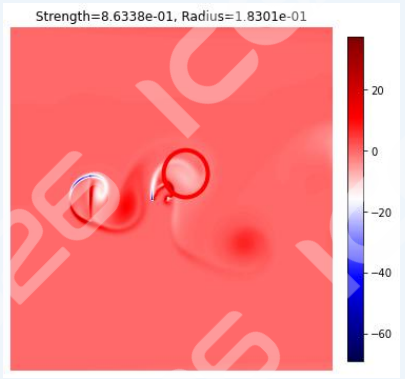
Case study · Where the model works and where it fails

0.55–0.95 · $R^2 \approx 0.64$



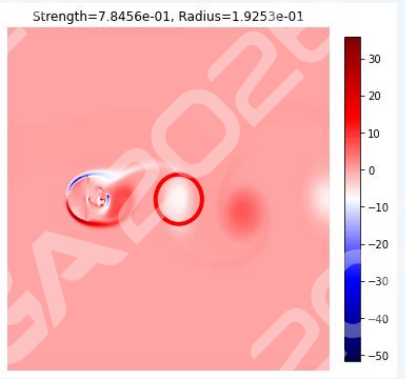
- Periodic wake, regular Kármán street
- Gentle flag motion (curvature 0.208)
- No disturbed gap in the band

1.55–1.95 · $R^2 \approx 0.71$



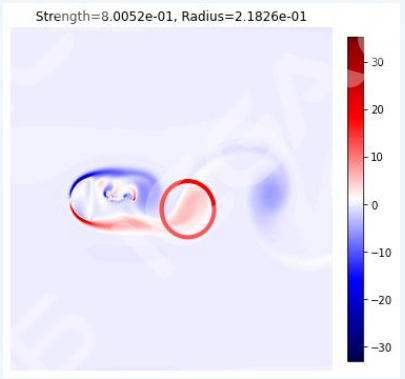
- Decayed wake: weakest vortices
- Single dominant flapping frequency (FFT at 1.8)
- Best case 1.55: R^2 0.80, loss 39 %

0.05–0.50 · $R^2 \approx 0.22$



- Flag inside the near wake
- Largest deformation (curvature 0.274)
- Gaps 0.20, 0.40 dropped; loss > 100 %

1.05–1.50 · $R^2 \approx 0.48$

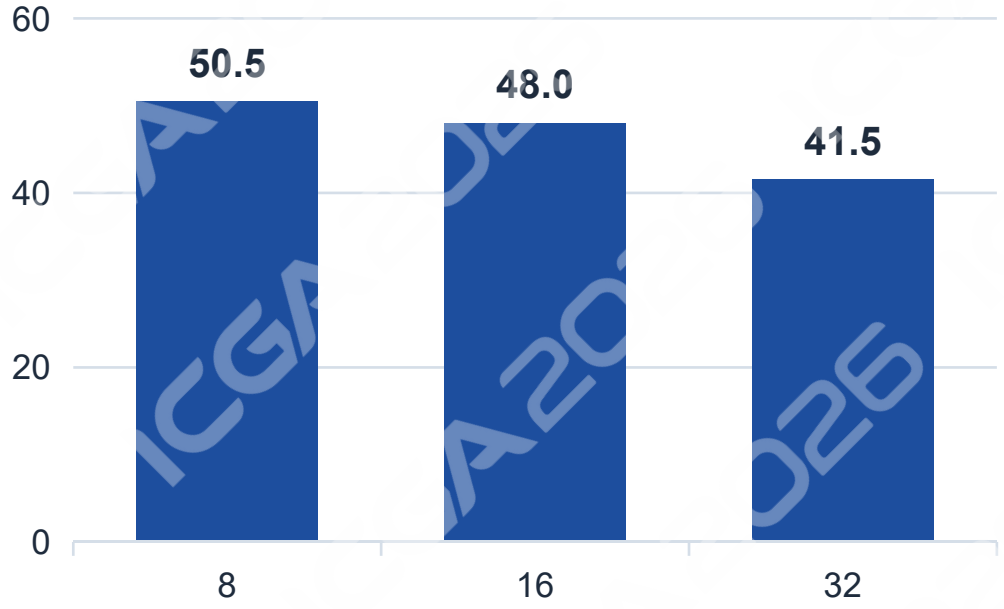


- Strongest vortices hit the flag
- Transitional band with disturbed gap 1.20
- Worst point 1.15: R^2 0.37

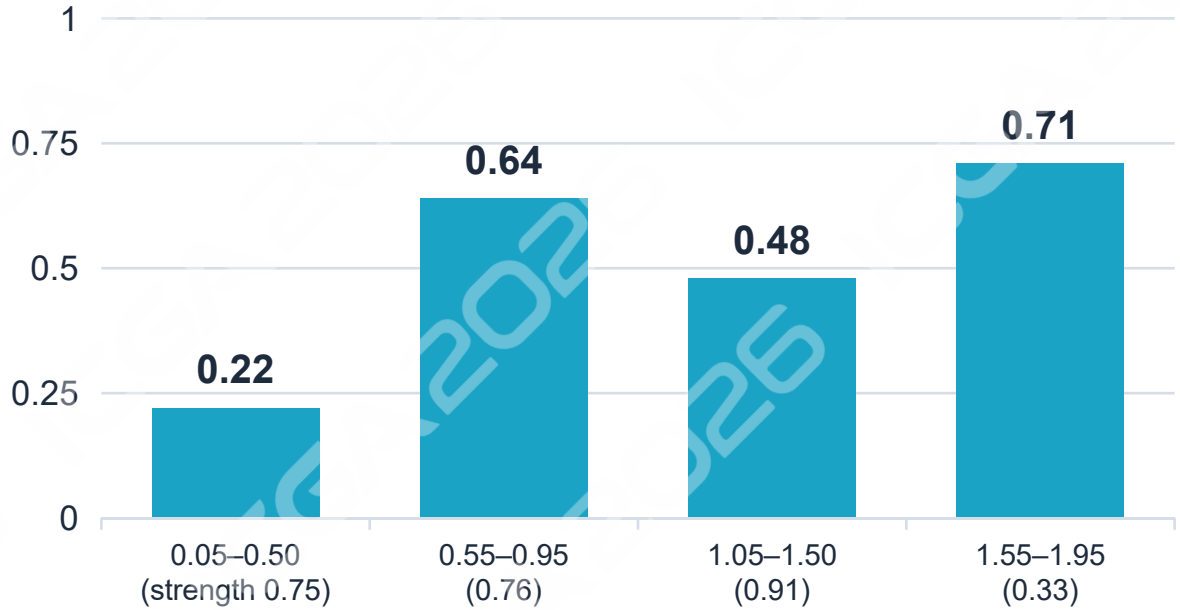
Red circle = tracked vortex.

Case study · Sensitivity to network width and vortex strength

Test loss vs. first-layer channels

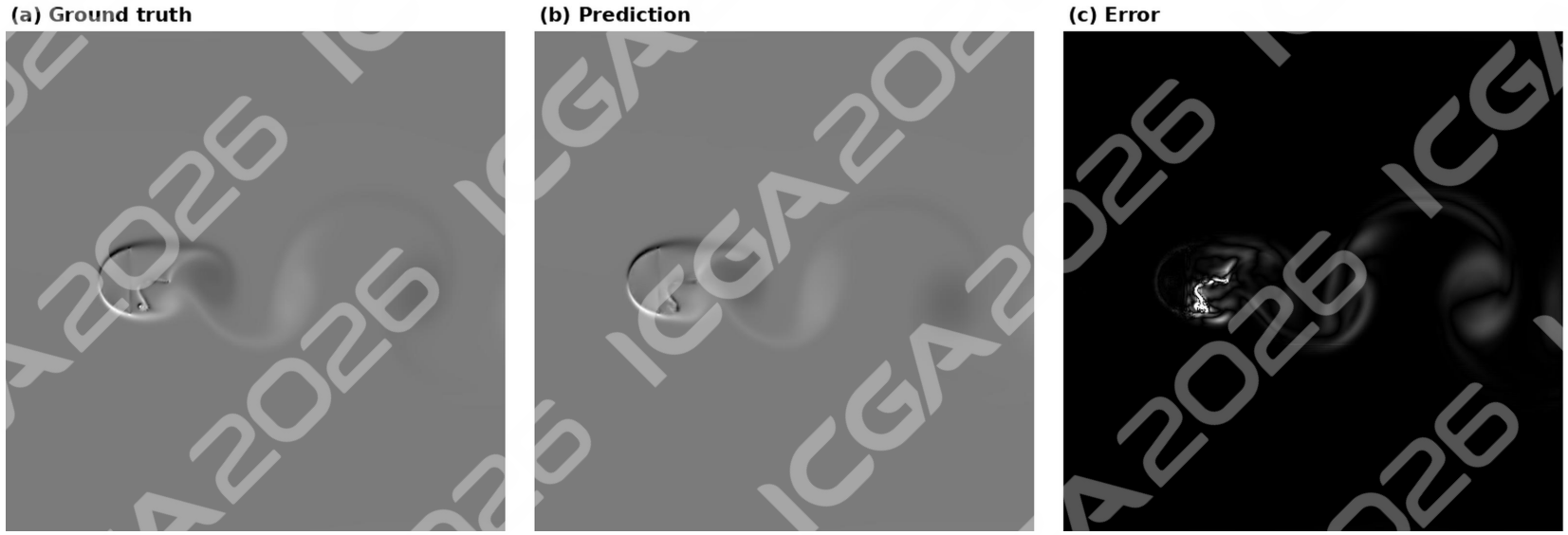


R^2 by gap band (avg. vortex strength)



More channels → lower loss up to 32; vortex strength alone does not decide accuracy: the flow regime does.

Case study · Where is the error concentrated?



Where

Largest discrepancies near the flag and its trailing region.

Why

High curvature and vortex–flag collisions create sharp local features.

Next

Flag-weighted loss (mask or signed distance) and temporal context.

Case study · Key findings

Regime-dependent skill

Works in periodic and decayed wakes (R^2 0.64–0.71); fails in the near wake and the transitional band.

Data coverage matters

The weakest bands contain the disturbed gaps 0.20, 0.40 and 1.20, dropped from the data.

The error lives at the flag

Discrepancies cluster around the flag where curvature and vortex impingement are highest.

One score hides the spread

Pooled R^2 0.80, but per-gap R^2 0.12–0.80 (mean ≈ 0.5); report the per-gap picture.

Outlook · From a canonical case to aviation problems

Now	Next	Then	Later	Goal
2D flag in a bluff-body wake, Re = 300; periodic wakes reconstructed well	More data near disturbed gaps; flag-weighted loss; ConvLSTM for transitional regimes	3D, higher Re, airfoil and flexible-wing geometries (Thuerey et al., 2020; Hickner et al., 2021)	Assimilate sensor data in a digital twin (Tuegel et al., 2011; Gao & Jaiman, 2024)	Design and monitoring loops for green-aviation systems

Each step needs new data, uncertainty estimates and validation against high-fidelity or measured references before design use.

Outlook · Limitations and open challenges

Limitations of this study

- Regime-dependent: weak in near-wake and transitional gaps
- Gaps 0.20, 0.40, 1.20 missing from the data
- Frame-wise, no memory; 2D, Re = 300
- Inference time not yet benchmarked

Next steps

- ConvLSTM or other temporal models
- Flag-weighted loss (mask or signed distance)
- More frames near the disturbed gaps
- 3D flows and higher Reynolds numbers

Take-home messages

- Net-zero aviation needs faster, trustworthy analysis of coupled flow–structure problems.
- Machine learning is moving from rigid-body flows to fluid–structure systems: PINNs, graph models, CNN surrogates.
- Masks + a gap-conditioned U-Net reconstruct wakes behind a flapping flag: pooled R^2 0.80, but 0.12–0.80 per gap.
- A pathway to aviation geometries and digital twins exists; validation and uncertainty remain the work ahead.

Thank you

Questions and discussion

References (1/5)

Abdelkefi, A. (2016). Aeroelastic energy harvesting: A review. *Int. J. Eng. Sci.* 100, 112–135.

Allen, J.J., Smits, A.J. (2001). Energy harvesting eel. *J. Fluids Struct.* 15, 629–640.

Amsallem, D., Farhat, C. (2008). Interpolation method for adapting reduced-order models and application to aeroelasticity. *AIAA J.* 46, 1803–1813.

Bearman, P.W. (1984). Vortex shedding from oscillating bluff bodies. *Annu. Rev. Fluid Mech.* 16, 195–222.

Bhatnagar, S., Afshar, Y., Pan, S., Duraisamy, K., Kaushik, S. (2019). Prediction of aerodynamic flow fields using convolutional neural networks. *Comput. Mech.* 64, 525–545.

Brunton, S.L., Noack, B.R., Koumoutsakos, P. (2020). Machine learning for fluid mechanics. *Annu. Rev. Fluid Mech.* 52, 477–508.

Bryant, M., Garcia, E. (2011). Modeling and testing of a novel aeroelastic flutter energy harvester. *J. Vib. Acoust.* 133(1), 011010.

Bukka, S.R., et al. (2021). Assessment of unsteady flow predictions using hybrid deep learning based reduced-order models. *Phys. Fluids*.

Cai, S., Mao, Z., Wang, Z., Yin, M., Karniadakis, G.E. (2021). Physics-informed neural networks (PINNs) for fluid mechanics: a review. *Acta Mech. Sin.* 37, 1727–1738.

Causin, P., Gerbeau, J.F., Nobile, F. (2005). Added-mass effect in the design of partitioned algorithms for fluid–structure problems. *Comput. Methods Appl. Mech. Eng.* 194, 4506–4527.

Cheng, C., et al. (2021). Deep learning based on PINN for solving 2 DOF vortex induced vibration of cylinder. *Ocean Eng.*

Chourdakis, G., Davis, K., Rodenberg, B., et al. (2022). preCICE v2: A sustainable and user-friendly coupling library. *Open Res. Europe* 2, 51.

Dowell, E.H., Hall, K.C. (2001). Modeling of fluid–structure interaction. *Annu. Rev. Fluid Mech.* 33, 445–490.

Duraisamy, K., Iaccarino, G., Xiao, H. (2019). Turbulence modeling in the age of data. *Annu. Rev. Fluid Mech.* 51, 357–377.

References (2/5)

Farea, A., Khan, S., Daryani, R., Ersan, E.C., Celebi, M.S. (2025). Learning fluid-structure interaction with physics-informed machine learning and immersed boundary methods. arXiv:2505.18565.

Fukami, K., Fukagata, K., Taira, K. (2019). Super-resolution reconstruction of turbulent flows with machine learning. *J. Fluid Mech.* 870, 106–120.

Gao, R., Jaiman, R.K. (2024). Predicting fluid-structure interaction with graph neural networks. *Phys. Fluids* 36, 013622.

Glaessgen, E., Stargel, D. (2012). The digital twin paradigm for future NASA and U.S. Air Force vehicles. *53rd AIAA/ASME/ASCE/AHS/ASC SDM Conf.*, AIAA 2012-1818.

Guo, X., Li, W., Iorio, F. (2016). Convolutional neural networks for steady flow approximation. *Proc. ACM SIGKDD*, 481–490.

Gupta, R., Jaiman, R. (2022). A hybrid partitioned deep learning methodology for moving interface and fluid–structure interaction. *Comput. Fluids*.

Hasegawa, K., Fukami, K., Murata, T., Fukagata, K. (2020). Machine-learning-based reduced-order modeling for unsteady flows around bluff bodies of various shapes. *Theor. Comput. Fluid Dyn.* 34, 367–388.

Hickner, M.A., et al. (2021). Data-driven unsteady aeroelastic modeling for control. arXiv:2111.11299.

Hou, G., Wang, J., Layton, A. (2012). Numerical methods for fluid-structure interaction: a review. *Commun. Comput. Phys.* 12, 337–377.

ICAO (2022). Long-term global aspirational goal (LTAG): net-zero CO_2 emissions from international aviation by 2050. 41st ICAO Assembly, Montréal.

Kim, D., Cossé, J., Huertas Cerdeira, C., Gharib, M. (2013). Flapping dynamics of an inverted flag. *J. Fluid Mech.* 736, R1.

Kingma, D.P., Ba, J. (2015). Adam: A method for stochastic optimization. *ICLR*.

Kochkov, D., Smith, J.A., Alieva, A., et al. (2021). Machine learning–accelerated computational fluid dynamics. *Proc. Natl. Acad. Sci. USA* 118, e2101784118.

Kohl, G., Chen, L.-W., Thuerey, N. (2023). Benchmarking autoregressive conditional diffusion models for turbulent flow simulation. arXiv:2309.01745.

References (3/5)

Kou, J., Zhang, W. (2021). Data-driven modeling for unsteady aerodynamics and aeroelasticity. *Prog. Aerosp. Sci.* 125, 100725.

Kutz, J.N. (2017). Deep learning in fluid dynamics. *J. Fluid Mech.* 814, 1–4.

Latif, U., Umar, H., Uddin, E., Akber, M. (2023). Computational analysis of inverted flag-based energy harvester in the wake of cylindrical bluff body. *Ocean Eng.* 281, 114920.

Lee, S., You, D. (2019). Data-driven prediction of unsteady flow over a circular cylinder using deep learning. *J. Fluid Mech.* 879, 217–254.

Lee, D.S., Fahey, D.W., Skowron, A., et al. (2021). The contribution of global aviation to anthropogenic climate forcing for 2000 to 2018. *Atmos. Environ.* 244, 117834.

Li, Z., Kovachki, N., Azizzadenesheli, K., et al. (2021). Fourier neural operator for parametric partial differential equations. *ICLR*.

Lino, M., Pfaff, T., Thuerey, N. (2025). Learning distributions of complex fluid simulations with diffusion graph networks. *ICLR*.

Livne, E. (2018). Aircraft active flutter suppression: State of the art and technology maturation needs. *J. Aircraft* 55(1).

Lu, L., Jin, P., Pang, G., Zhang, Z., Karniadakis, G.E. (2021). Learning nonlinear operators via DeepONet. *Nat. Mach. Intell.* 3, 218–229.

Lucia, D.J., Beran, P.S., Silva, W.A. (2004). Reduced-order modeling: new approaches for computational physics. *Prog. Aerosp. Sci.* 40, 51–117.

Lusch, B., Kutz, J.N., Brunton, S.L. (2018). Deep learning for universal linear embeddings of nonlinear dynamics. *Nat. Commun.* 9, 4950.

Mathieu, M., Couprie, C., LeCun, Y. (2016). Deep multi-scale video prediction beyond mean square error. *ICLR*.

Michelin, S., Doaré, O. (2013). Energy harvesting efficiency of piezoelectric flags in axial flows. *J. Fluid Mech.* 714, 489–504.

Miyanawala, T.P., Jaiman, R.K. (2019). A hybrid data-driven deep learning technique for fluid-structure interaction. arXiv:1807.09591.

References (4/5)

Murata, T., Fukami, K., Fukagata, K. (2020). Nonlinear mode decomposition with convolutional neural networks for fluid dynamics. *J. Fluid Mech.* 882, A13.

Nazvanova, A., et al. (2023). A data-driven reduced order model based on long short-term memory neural network for vortex-induced vibrations of a circular cylinder. *Phys. Fluids*.

Ong, M.C., Yin, G. (2025). Synergizing machine learning with fluid–structure interaction research: An overview of trends and challenges. *Ocean* 1, 9470002.

Parekh, A.R., Gao, R., Jaiman, R.K. (2025). An efficient and accurate surrogate modeling of flapping dynamics in inverted elastic foils using hypergraph neural networks. arXiv:2511.22012.

Perez, E., Strub, F., de Vries, H., Dumoulin, V., Courville, A. (2018). FiLM: Visual reasoning with a general conditioning layer. *AAAI* 32, 3942–3951.

Peskin, C.S. (2002). The immersed boundary method. *Acta Numer.* 11, 479–517.

Pfaff, T., Fortunato, M., Sanchez-Gonzalez, A., Battaglia, P.W. (2021). Learning mesh-based simulation with graph networks. *ICLR*.

preCICE tutorials (precice.org; github.com/precice/tutorials), FSI cases and figures: LGPL-3.0.

Raissi, M., Wang, Z., Triantafyllou, M.S., Karniadakis, G.E. (2019a). Deep learning of vortex-induced vibrations. *J. Fluid Mech.* 861, 119–137.

Raissi, M., Perdikaris, P., Karniadakis, G.E. (2019b). Physics-informed neural networks. *J. Comput. Phys.* 378, 686–707.

Raissi, M., Yazdani, A., Karniadakis, G.E. (2020). Hidden fluid mechanics: Learning velocity and pressure fields from flow visualizations. *Science* 367, 1026–1030.

Ronneberger, O., Fischer, P., Brox, T. (2015). U-Net: Convolutional networks for biomedical image segmentation. *MICCAI*, LNCS 9351, 234–241.

Rowley, C.W., Dawson, S.T.M. (2017). Model reduction for flow analysis and control. *Annu. Rev. Fluid Mech.* 49, 387–417.

Sader, J.E., Cossé, J., Kim, D., Fan, B., Gharib, M. (2016). Large-amplitude flapping of an inverted flag in a uniform steady flow: a vortex-induced vibration. *J. Fluid Mech.* 793, 524–555.

References (5/5)

Sanchez-Gonzalez, A., Godwin, J., Pfaff, T., et al. (2020). Learning to simulate complex physics with graph networks. *ICML*, PMLR 119, 8459–8468.

Schmid, P.J. (2010). Dynamic mode decomposition of numerical and experimental data. *J. Fluid Mech.* 656, 5–28.

Shoele, K., Mittal, R. (2016). Energy harvesting by flow-induced flutter in a simple model of an inverted piezoelectric flag. *J. Fluid Mech.* 790, 582–606.

Taira, K., Brunton, S.L., Dawson, S.T.M., et al. (2017). Modal analysis of fluid flows: An overview. *AIAA J.* 55, 4013–4041.

Tang, H., et al. (2022). A transfer learning-physics informed neural network (TL-PINN) for vortex induced vibration. *Ocean Eng.*

Thuerey, N., Weißenow, K., Prantl, L., Hu, X. (2020). Deep learning methods for Reynolds-averaged Navier–Stokes simulations of airfoil flows. *AIAA J.* 58, 25–36.

Thuerey, N., Holl, P., Mueller, M., Schnell, P., Trost, F., Um, K. (2021). Physics-based deep learning. arXiv:2109.05237; open-access book, physicsbaseddeeplearning.org (figures: Apache-2.0).

Tuegel, E.J., Ingraffea, A.R., Eason, T.G., Spottswood, S.M. (2011). Reengineering aircraft structural life prediction using a digital twin. *Int. J. Aerosp. Eng.* 2011, 154798.

Turek, S., Hron, J. (2006). Proposal for numerical benchmarking of fluid–structure interaction between an elastic object and laminar incompressible flow. In: Bungartz, H.-J., Schäfer, M. (eds) *Fluid-Structure Interaction: Modelling, Simulation, Optimisation*, LNCSE 53, Springer, 371–385.

Vinuesa, R., Brunton, S.L. (2022). Enhancing computational fluid dynamics with machine learning. *Nat. Comput. Sci.* 2, 358–366.

Williamson, C.H.K., Govardhan, R. (2004). Vortex-induced vibrations. *Annu. Rev. Fluid Mech.* 36, 413–455.